

FLIGHT ROTOR LOADS CALCULATION: MULTIPLE PATH APPROACH

Dr. Ermanno Fosco

Senior engineer, Structural Dynamics Dept.
ermanno.fosco@agustawestland.com

Dr. Attilio Colombo

Head of Structural Dynamics Dept.
attilio.colombo@agustawestland.com

Dr. Francesco Vincenzo

Engineer, Structural Dynamics Dept.
francesco.vincenzo@agustawestland.com

Dr. Claudio Monteggia

Head of Rotor Dynamics and Loads Dept.
claudio.monteggia@agustawestland.com

Dr. Pierre Abdel Nour

Head of Vehicle Technologies and Aeromechanics
pierre.abdelnour@agustawestland.com
AgustaWestland, C. Costa di Samarate, Varese, Italy

Mr. Nicholas Griffiths

Specialist, Rotor Dynamics and Loads Dept.
nicholas.griffiths@agustawestland.com

Dr. Chris Hutchin

Analyst, Rotor Dynamics and Loads Dept.
chris.r.hutchin@agustawestland.com

AgustaWestland, Yeovil, Somerset, United Kingdom

ABSTRACT

Many factors contribute to define the competitiveness of a complex product as a helicopter and the knowledge of the aspects which control these factors is essential to address the company efforts in the correct way. In this context, the importance of factors such as comfort, fatigue and performances is undoubted for modern helicopters, as well as the knowledge of the parameters which can affect them.

On this subject, measurements of rotor loads become very useful information, since the rotor represents the principal source of vibrations and fatigue issues, as well as his behaviour determines the performances of the aircraft.

The inference of flight rotor loads, both static and dynamic, especially if related to the complete set of them, has always been very difficult to achieve, being arduous to find a proper location close to the rotor where putting the sensors in an effective way for the estimation of all the loads.

The aim of this paper is to present different methodologies used to approach the problem of rotor loads measurements and integrate them, in order to reconstruct the complete set of loads at the hub. These procedures arise from the employment of different measurements on multiple structural load paths. In fact, only using a complete set of data and phasing the different contributions in a unique dynamic assessment, the methodology can provide the information needed to properly evaluate the loads transferred to the helicopter fuselage, improving the accuracy and robustness of the results by cross-checking the available information.

On this subject, the investigation involves sensors installed in different locations, as rotor shaft, main gearbox struts, hub component and rotor blades; the acquisition includes not only strain gauges, but also accelerometers and potentiometers, in order to measure respectively hub accelerations and blades motion. The integration of all the aforementioned kind of measurements has been carried out and properly optimized, in order to assess an overall systematic methodology.

Such a methodology is easily applicable to helicopters which show similar configuration for rotor (articulated architecture) and gear-box installations, but could be extended, with some modifications, to different layouts.

As result of this activity, the complete set of main rotor loads, both static and vibratory, has been derived for the complete envelope of level flight conditions; however, this approach is valid for all the stabilized flight conditions and can be easily adapted in order to manage also data related to maneuvers.

Moreover, the acquisition of measurements directly on main rotor blades, together with some contributions from analytical evaluations, allows inferring the amount of forces at blade hinge in the rotating axis system. In conjunction with the measured hub data, these results provide the starting point for highlighting which are the important factors on the blade dynamic behavior in relation to the rotor loads generation process.

The indications coming from these results can be very useful to define which are the most critical loads in terms of resultant comfort and fatigue spectrum related to the different flight conditions. Moreover, they can also provide further detailed design criteria and give useful indications on the effectiveness of the design related to the installation of anti-vibration devices. All these information will be very helpful for the development of the new generation helicopters, by allowing to obtain high performances with low vibratory excitations.

INTRODUCTION

Many factors contribute to define the competitiveness of a complex product as a helicopter and the knowledge of the aspects which control these factors is essential to address the company efforts in the correct way. In this context, the importance of factors such as comfort, fatigue and performances is undoubted for modern helicopters, as well as the knowledge of the parameters which can affect them. On this subject, the comprehension of aircraft performances and comfort needs to start from rotor component and its loads generation.

The inference of flight rotor loads, especially if related to the complete set of them, has always been very difficult to achieve, being arduous to find a valid area close to the rotor to put the sensors in an effective way for the calculation of all the loads; at this proposal, the investigation here reported involved sensors installed in different locations, as rotor shaft, main gearbox struts, hub component and rotor blades; the acquisition includes not only strain gauges, but also accelerometers and potentiometers, in order to measure respectively hub accelerations and blades motion.

The integration of all the aforementioned kind of measurements has been carried out and properly optimized, in order to assess an overall systematic methodology and add reliability to the final load results.

Such a methodology is easily applicable to helicopters which show similar architecture for rotor and gear-box installations, but could be extended, with some modifications, to different layouts.

The loads identification process described in this paper includes improvements, with respect to the past AgustaWestland approach, related to different aspects, as new instrumentation layout, enhanced calibration procedures and improved calculation methodologies. The results obtained as consequence of this new assessment seem to be, on the whole, quite consistent and highlight some significant indications on rotor excitations entity and loads sharing.

These results could be further improved, especially concerning their accuracy and reliability, by adding some calibration features, not presently implemented for budget and time constraints: on this subject, possible enhancement have been identified during the performed job, have been highlighted in this paper and would represent the core of a future continuation work.

MULTIPLE LOADS PATH MEASUREMENTS

The proposed loads identification methodology is based on the processing of the measurements coming from multiple load paths (see *Figure 1*).

Particularly, the investigation has been focused on the following components:

- mast/MGB struts assembly, that provides a direct measure of the almost full loads set coming from the rotor and transferred to the helicopter fuselage
- rotor hub, which allows estimating beam and chord bending forces at reference blade hinge by using new instrumentation layout, less sensitive with respect to centrifugal force

- rotor blade, which provides the resulting forces acting at the hinge, starting from measurements acquired using 2/ bending bridges installed along the blade axis

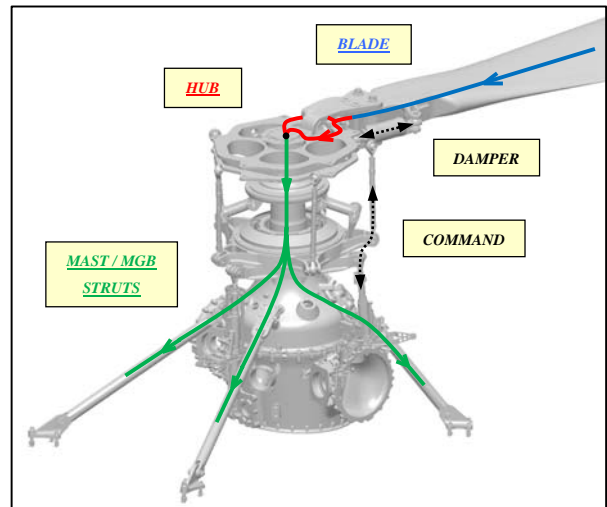


Figure 1: Multiple loads path measurements

In addition, being damper and command loads further elements in the scheme of overall forces acting on the interface between rotor and fuselage, they have been included into the calculation process.

The employment of different load paths has been pursued in order both to provide enough data for the full hub loads set calculation and to improve accuracy and robustness of the final results by cross-checking the available information.

Moreover, the acquisition of measurements directly on main rotor blades, together with some contributions from analytical evaluations, allows inferring the amount of forces at blade hinge, though providing useful information about the key-factors involved in the rotor loads generation process.

For what concern the improvements applied to the different procedures, the details will be shown in the next paragraph; nevertheless, a summary of the modifications introduced for mast and hub load paths is the following:

PROCEDURE & CALCULATION IMPROVEMENTS	
Mast:	
1.	Addition of a third couple of shaft bending bridges
2.	Combined processing of mast and MGB struts sensors in order to add accuracy
3.	Definition of a calibration procedure directly on the helicopter
Hub:	
1.	New instrumentation layout for loads sensitivity optimization
2.	Determination by test of the full sensitivity matrix in place of the conventional calibration procedure
3.	Development of an analytical tool to infer the hub loads set, basing on the periodicity of the rotor

MAST SENSOR LAYOUT & CALIBRATION SET-UP

The M/R mast sensors set is normally composed, for an AgustaWestland prototype helicopter, by two couples of bending bridges, act to measure moments out of the rotor plane (along two orthogonal directions), and a torque sensor, which provides information about the moment in the rotor plane. The use of an additional axial sensor (along the shaft axis) is usually avoided, being his accuracy quite low due to the very high stiffness of the mast in this direction.

The employment of one couple of bending sensors for each direction, with strain gauges at two different positions along the shaft axis, provides the minimum required information for shears (rotor in-plane) and moments (rotor out-plane) calculation.

For the investigation here proposed, as one of the applied improvements, the two couples of bending bridges have been incremented with one more strain gauge for each direction, in an intermediate location between the existing two. This new configuration leads improving the accuracy of the calculation procedure, given that the local constraints don't allow achieving an optimal amount of distance between upper and lower couples of strain gauges.

The other important issue of this elaboration is related to the methodology used for the calibration of these sensors, considering that the strain gauges, especially concerning the upper ones, are very close to the hub/mast clamping area; this consideration led questioning the traditional calibration made by applying a transversal force on the shaft component itself, without taking into account any clamping effects.

For this reason, a dedicated "on field" calibration has been made directly on the helicopter in ground, without main rotor blades but with the other rotor components fully installed.

The calibration loads have been applied by means of known incremental weights, introduced at the tip of a dummy blade (short part of a blade provided with bushings at its tip) installed in turn at different rotor azimuths. With this procedure, the static forces introduce both axial loads (no shears are generated, provided that shaft component is vertical) and, more important for present activity, bending moments at the mast component, allowing to evaluate the corresponding measurements at the sensors of interest.

This calibration procedure highlighted some accuracy problems, due to the low repeatability of the test for its implicit "on field" characteristic, but allowed to underline the entity of errors made with the standard calibration procedure.

Results are in the diagram shown in *Figure 2* for upper, middle and lower bridges and in correspondence of a few similar tests (different azimuths, repeated tests, etc...), in terms of correction factors between helicopter tests and standard calibration (coefficient = 1.0 means no differences): the outcome of this comparison is a discrepancy which is quite small for the middle bridges (green line) but is relevant for upper and lower strain gauges.

Particularly, the errors between tests and standard calibration for the upper bridges (blue line), which are very close to the hub/mast clamping area, exhibit values up to 10% of the measured data.

The final set of correction factors, taken as reference for all the rotor load calculations, has been derived as average of the aforementioned tests and consists in the following values:

1.07 for BB1 (upper sensors), 0.92 for BB2 (lower bridges) and 0.98 for BB3 (strain gauges in the middle).

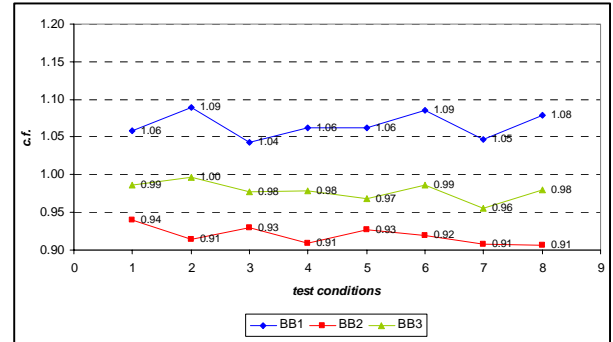


Figure 2: Mast bridges correction factors

MAST DATA PROCESSING

The processing of each signal acquired during the loads identification flights has been based on its harmonic decomposition and for this purpose a dedicated harmonic fitting procedure has been set-up.

Since the complete set of data contains signals both in fixed and rotating frames and the final load results are mainly required in the helicopter coordinate system, all the rotating parameters have been projected in this last reference [1]. Particularly, by means of the "marker" sensor position, the time histories of all the parameters involved in the loads calculation have been expressed in a unique reference phase, in order to couple them in a consistent way. An example related to the transformation of the mast bending signals from rotating frame to the reference helicopter system, focalized on the main N/rev contribution ($[N-1]/rev$ and $[N+1]/rev$ in the rotating frame), is shown in *Figure 3*.

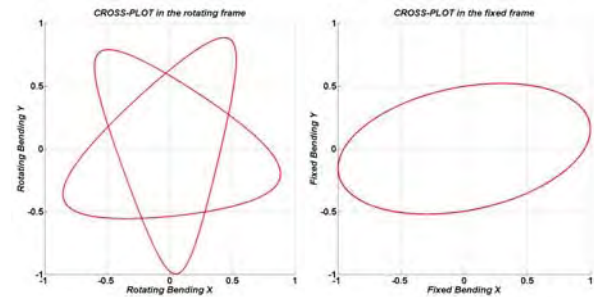


Figure 3: Rotating-fixed frame transformation

Starting from the signals elaboration described so far, the methodology for rotor loads calculation is based on the two following relationships:

- bending moment equilibrium equations for all the instrumented mast stations
- consistency between measured MGB strut axial forces and expected loads, calculated as result of analytical transfer functions between hub and strut loads

The resulting equations, written in terms of real and imaginary parts (i.e. harmonic components described with the complex notation) make up the following linear system:

$$\begin{bmatrix} [h] & [0] & -\text{Re}([B]) \\ [0] & -[h] & \text{Im}([B]) \\ \text{Re}([F]) & -\text{Im}([F]) & [0] \\ \text{Im}([F]) & \text{Re}([F]) & [0] \end{bmatrix} \begin{Bmatrix} \text{Re}(\{x\}) \\ \text{Im}(\{x\}) \\ \alpha \\ \beta \\ \gamma \end{Bmatrix} = \begin{Bmatrix} \{0\} \\ \text{Re}(\{C\}) \\ \text{Im}(\{C\}) \end{Bmatrix}$$

where the first two rows refer to the equilibrium equations, related to each n^{th} harmonic contribution, while the last two define the relationships between hub loads and MGB rods thrust. The reported matrices are:

$$[B] = \begin{bmatrix} BB1_{xfn} & 0 & 0 \\ 0 & BB2_{xfn} & 0 \\ 0 & 0 & BB3_{xfn} \\ BB1_{yfn} & 0 & 0 \\ 0 & BB2_{yfn} & 0 \\ 0 & 0 & BB3_{yfn} \end{bmatrix}$$

which represents bending measurements for both X_f and Y_f directions (fixed reference system) at the selected n^{th} harmonic.

$$[h] = \begin{bmatrix} h_1 & 0 & 1 & 0 & 0 & 0 \\ h_2 & 0 & 1 & 0 & 0 & 0 \\ h_3 & 0 & 1 & 0 & 0 & 0 \\ 0 & h_1 & 0 & 1 & 0 & 0 \\ 0 & h_2 & 0 & 1 & 0 & 0 \\ 0 & h_3 & 0 & 1 & 0 & 0 \end{bmatrix}$$

which includes the geometrical positions of the different strain gauges.

The transfer function matrix [F], deriving from FE analysis, defines the relationship between hub loads and MGB rods thrust; the analytical approach has also been employed for the command loads contribution, through the matrix [F_{com}], which represents the transfer functions between the three servo forces (F_{Zi}) and the strut axial loads.

The introduction of this load path is needed in order to have the correct sharing between rotor and command loads on the strut measurements, as stated below:

$$\{C\} = \begin{Bmatrix} C1_n \\ C2_n \\ C3_n \\ C4_n \end{Bmatrix} = \begin{Bmatrix} \overline{C1}_n \\ \overline{C2}_n \\ \overline{C3}_n \\ \overline{C4}_n \end{Bmatrix} - [F_{com}] \begin{Bmatrix} -F_{Z1} \\ -F_{Z2} \\ -F_{Z3} \end{Bmatrix}$$

where the vector $\{\overline{C1}_n \dots \overline{C4}_n\}^T$ represents the original strut acquisitions, while {C} has been corrected with servo contributions.

Finally, the coefficients α , β and γ are the correction factors of M/R bending measurements defined before and the unknown vector {x}:

$$\{x\} = \{S_{xfn} \ S_{yfn} \ M_{yfn} \ M_{xfn} \ M_{zfn} \ S_{zfn}\}^T$$

represents the n^{th} contribution of the hub loads in the fixed frame.

By fixing the value of torque moment M_{zfn} (directly measured by means of the dedicated sensor) and the set of correction factors α , β and γ , the resulting hub loads in the fixed frame can be calculated by solving the *constrained linear least-square problem* reported above.

This methodology has been employed both for dynamic and static calculations: particularly, in this last case, the real part in the previous equations has been set equal to the static value, while the imaginary one is zero.

An example of the matching between the different measurements and the reconstruction obtained by solving the least-square system is shown in the next polar diagram (see *Figure 4*), related to the n^{th} harmonic components for an analyzed flight condition.

In details, the list of the plotted data is:

- M/R mast bending bridges
 - X_f direction (blue arrow)
 - Y_f direction (red arrow)
 - Measured data (thick arrow)
 - Calculated data (dotted arrow)
- MGB struts thrust
 - Strut n° 1 - forward left (blue arrow)
 - Strut n° 2 - forward right (cyan arrow)
 - Strut n° 3 - aft left (red arrow)
 - Strut n° 4 - aft right (magenta arrow)
 - Measured data (thick arrow)
 - Calculated data (dotted arrow)

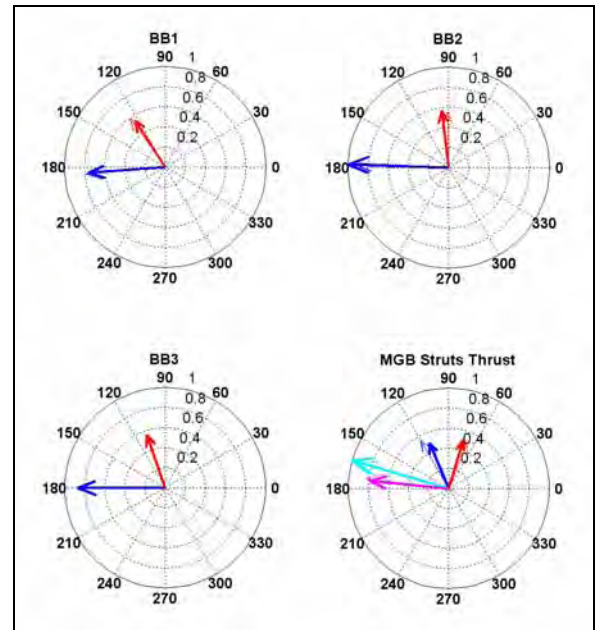


Figure 4: Polar diagram comparison

These diagrams highlight very small differences between measured and reconstructed data, concerning amplitudes and phases of both shaft moments and strut loads. The use of the struts information, in addition to the conventional approach based on shaft data only, allows improving the accuracy of the results, which normally is affected by the very low distance existing between bending sensors. Moreover, the rotor thrust load cannot be calculated only by using mast measurements, because of the stiffness problem mentioned before.

Notice that, if the contribution of the struts coupling is removed from the system solving (struts information used for thrust calculation only), the hub load results are not able to properly reconstruct all the measured strut forces; in this case, matching of bending shaft data is further improved (comparison on BBi remains acceptable also in the full coupled case, as visible in previous plot) but, even though the order of magnitude of the strut loads is caught, some errors in phase can be found.

The same considerations can be made for static loads calculation, which exhibit similar characteristics on matching of reconstructed amplitudes (in this case no phases are involved).

HUB SENSORS LAYOUT AND CALIBRATION PROCEDURE

Hub component has a quite complex shape, which doesn't help to configure a valid instrumentation set-up and furthermore it is particularly affected by the blade centrifugal forces, which are normally dominant on the overall rotor loads, either static or vibratory contributions.

Taking into account these remarks, an analytical optimization of sensor locations has been performed, in order to minimize the effect of centrifugal forces, as well as to reduce coupling between different load contributions, coming from main rotor blades (flapwise, chordwise and centrifugal forces), on the acquired data.

On the light of FEM simulations, a hypothesis of sensors configuration, compliant with previous requirements and compatible with installation constraints, has been verified by test on experimental instrumentation, leading to employ a set of 4 bridges. This instrumentation set is made up of 1 TH bridge, optimized for centrifugal force measurements, 1 BB bridge, characterized by high sensitivity to beam bending loads and 2 CB bridges, configured so that to maximize response to chord bending forces (see *Figure 5*).

The duplication of CB sensors, actually located in different hub area, aims at providing a comparison for the most critical measures, due to the fact that such kind of bridges is particularly complex and partially sensitive to the other loads. Moreover, this redundancy could become necessary in case the entity of damper loads is able to affect hub measurements; in this case, damper loads would become an unknown inside the linear system to be solved, as explained below, and one more equation (provided by the matching with the added CB bridge) would result essential in order to make the problem solvable.

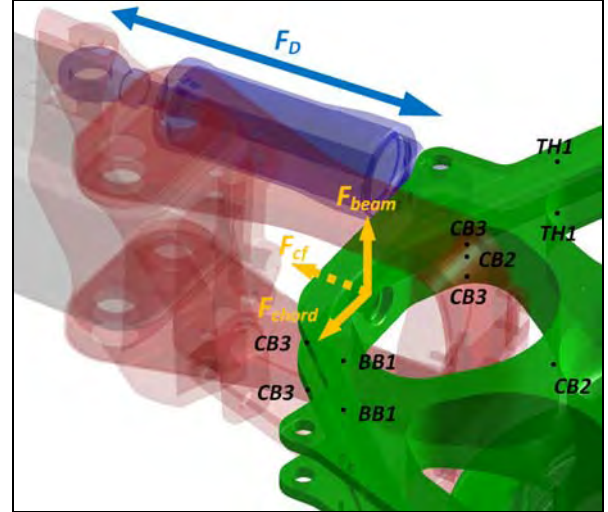


Figure 5: Hub sensors layout

Concerning sensors calibration, a dedicated test-rig has been set-up in order to be able to apply all the required loads. On this subject, a clarification is needed about the real meaning of the word “calibration”: in fact, being the cross-coupling terms between loads and sensors output not negligible for most of cases, the full populated matrix sensitivity has to be calculated. Moreover, consider that only one arm of the hub is instrumented, but the sensitivity between all the blade loads and the sensors output is required.

On the light of these considerations, in place of a “standard” calibration based on the collective loads only, performed tests included the application of all the forces on each blade, together with a radial collective pre-load equal to the nominal centrifugal force.

Notice that, because of the incompatibility of the test rig, radial loads have been applied in a collective way only; therefore, the available terms of the sensitivity matrix refer to the N -blades beam-bending and chord-bending forces only, in addition to the centrifugal force effect.

This approach is valid for articulated rotors only, being the moments transferred from blades to hub, through the elastomeric bearing components, negligible with respect to the other contributions.

The full sensitivity matrix, filled with the procedure described above, has the following structure:

	Loading Condition	BB1	CB2	CB3	TH1
	Collective chord bending	x	x	x	x
	Collective beam bending	x	x	x	x
{CFS}	Collective centrifugal force	x	x	x	x
{CS}	Chord bending force FC_1	x	x	x	x
	...	x	x	x	x
	Chord bending force FC_N	x	x	x	x
{BS}	Beam bending force FB_1	x	x	x	x
	...	x	x	x	x
	Beam bending force FB_N	x	x	x	x

Table 1: Hub strain gauges sensitivity matrix [mV/daN]

Concerning the damper loads sensitivity, the application of a suitable force (with amplitude similar to what expected during

flight) at damper interface points led to negligible effects in the entire set of sensor measurements: this result allowed to completely remove the related equations from the linear system.

The final standard calibration, used to set-up each bridges sensitivity for flight activities, is extracted from the collective loading part of the sensitivity matrix (highlighted values in *Table 1*): this set-up defines the output of the measurements, which will be then processed by an in-house code, in order to assess the hub loads calculation.

In order to associate the hub sensors output with the single forces acting at blade hinge, all the coefficients related to the single force application have been divided by the corresponding bridge standard calibrations.

Given $STANDARD_CAL_j$ as the calibration term of the j^{th} sensor, the coefficients of influence between the k^{th} hinge load and the output sensors become:

$$CB_CAL_{kj} = \frac{CS_{kj}}{STANDARD_CAL_j} \quad k = 1 \dots N$$

$$BB_CAL_{kj} = \frac{BS_{kj}}{STANDARD_CAL_j} \quad k = 1 \dots N$$

$$CF_CAL_j = \frac{CFS_j}{STANDARD_CAL_j}$$

Notice that $\{CF_CAL\}$ is a vector because it is associated to the only performed collective radial loading condition.

These coefficients will be directly employed in the data processing of the hub sensors, in order to calculate the required hinge loads.

M/R HUB DATA PROCESSING

Let consider an ideal rotor with its periodicity and let choose a reference blade that produces a generic force $F(t)$ at time instant t ; the corresponding force $F_k(t)$ generated by the k^{th} blade, which follows the reference one, can be expressed as [2]:

$$F_k(t) = F\left(t + (k-1)\frac{\Delta\psi}{\Omega}\right) \quad k = 1 \dots N$$

where $\Delta\psi$ represents the azimuth angle between two consecutive blades.

Following this approach, the force $F(t)$ defined above can be expressed as harmonic summation:

$$F(t) = F_0 + \sum_n F_n^C \cos(n\Omega t) + F_n^S \sin(n\Omega t)$$

Substituting this harmonic summation into the previous periodicity relationship, by considering Ωt as the rotor azimuth position ψ , the generic force generated by the k^{th} blade becomes:

$$F_k(\psi) = F_0 + \sum_n F_n^C \cos(n\psi + n(k-1)\Delta\psi) + F_n^S \sin(n\psi + n(k-1)\Delta\psi)$$

where:

- F_0 represents the static contribution to the force at reference blade hinge.

- F_n^C and F_n^S represent the n^{th} harmonic contributions to the force at reference blade hinge.

Measurements on the hub bridges can be written as a summation of each force acting on the N -blades by using the coefficients of influence contained in the previously defined matrices ($[BB_CAL]$, $[CB_CAL]$ and $\{CF_CAL\}$).

The resulting equations, combined with the harmonic summation defined above, lead to an over-determined linear system at constant coefficients. The solution of this system, calculated with a least-square standard approach, provided the harmonic contributions (static term included) for required forces at reference blade hinge.

Notice that this kind of approach, which infers all the blade dynamics from the only reference one (basing on the hypothesis of ideal behaviour of the rotor), is valid only if the periodicity assumption can be applicable to the analyzed flight conditions. Particularly, in this case only stabilized level flight conditions have been considered.

In order to evaluate the effectiveness of this methodology, being the linear system over-determined, it is useful looking at the differences between measured and reconstructed azimuth histories, which represent a graphical indication of the solution residual.

This comparison is reported, for a stabilized flight condition, in the following plot (*Figure 6*).

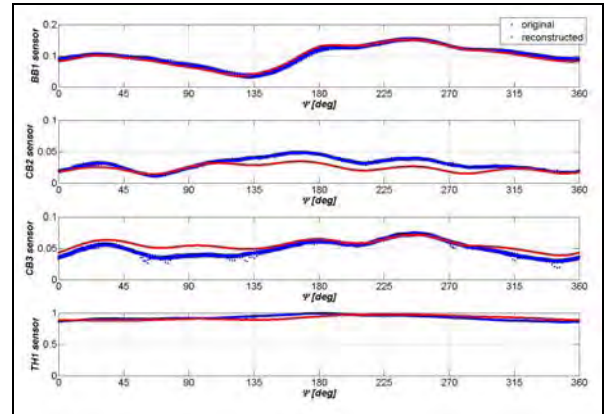


Figure 6: Hub sensors signal reconstruction

This diagram, showing the sensors time histories in terms of azimuth position for each rotor turn, highlights the following remarks:

- the comparison should be made on the overall set of sensors, since the selection of the adopted weighting matrix can modify the quality of the single signal reconstruction;
- however, with this normalization BB1 signal seems showing the best reconstruction, according with the fact, analyzed later in detail, that the missing radial force contribution probably causes small corrections to this measurement;
- static components show a general good agreement between measurements (blue curves) and reconstructed signals (red curves);

- dynamic components highlight some discrepancies, even if the order of magnitude of the reconstructed data is consistent with the acquired one.

On this last point, in order to better understand the dynamic comparison, the residual found for each main frequency contribution has been detailed in the next diagram, related to level flight at high speed (*Figure 7*).

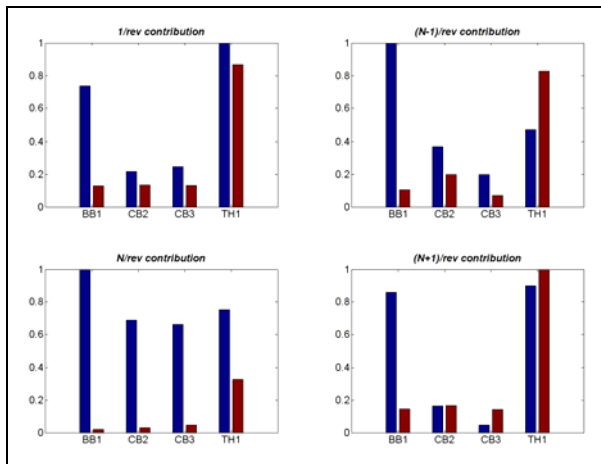


Figure 7: Solution residual for high speed condition

The plot above is subdivided for harmonic contributions $\{1/rev, (N-1)/rev, N/rev \text{ and } (N+1)/rev\}$ and each couple of bars refers to a single sensor; the blue bars are related to the harmonic measured amplitude, while the red ones refer to a residual error based both on amplitude and phase discrepancies (as norm of the difference vector between measured and reconstructed harmonic contributions).

The following considerations can be made:

- BB1 signal components show good agreement at all the compared frequencies, as anticipated for time history matching; this result will determine, as highlighted in the hub loads comparison paragraph, a predictable agreement in the out of plane rotor forces (and in-plane moments) reconstruction;
- in general, the N/rev component seems to be quite well reconstructed, except for TH1 sensor, which shows not negligible inconsistencies: this is probably due to the very low ratio between dynamic and static components, given that this sensor is more sensitive to centrifugal forces;
- on the contrary, $1/rev$, $(N-1)/rev$ and $(N+1)/rev$ harmonic components generally exhibit (with some BB1 exceptions) significant discrepancies: this is probably due, at least in part, to the absence of the radial force contribution, not included in the calculation because of test rig limitations.

A detailed investigation about this partial sensors mismatch will be deferred to the section concerning the hub loads comparison.

STRAIN MODAL SYNTHESIS ANALYSIS

Another fully independent method, employed for identifying the rotor loads set, but also important in order to infer the

unknown blade hinge forces, makes use of blade strain gauge data. This method is known as Strain Modal Synthesis (SMS) and involves a least-squares fit of predicted blade modal bending moments to match the measured blade strain gauge data.

This method does provide additional insight into the blade loading actions which generate vibratory loads and it is able to identify contributions from each blade mode in the rotating axes system. SMS cannot provide radial shears, which have to be calculated by alternative means. Modal methods in general cannot deal with the application of discrete loads such as that generated by the hydraulic lag damper. This limitation has been addressed with a unified formulation method which takes the form of a hybrid force integration/modal summation correction. Further limitations of SMS include a dependence on the accuracy of the calculated blade modes which are assumed to be constant with pitch and the quality of the fitting.

SMS methodology carries out modal fitting to the signals recorded by blade strain gauges during flight test; the software fits to a 10 harmonic Fourier representation of the input wave rather than the wave itself. Therefore, in order to allow the evaluation of the Fourier coefficients, a representative section of the data must be chosen.

This is completed in two steps: first, a steady section of data is chosen through visual inspection of the flight parameters, such as flight speed, altitude and vertical acceleration; then, a software utility is used to find three cycles of data that is repeatable and representative for all of the channels.

The elastic blade modes (together with rigid flap and lag), which are used in the mentioned calculation process, cannot be fit to the distribution resulting from the application of a discrete load, such as that from the lag damper. Since the damper load is an important and significant factor in the blade bending moments, some attempt has to be made to take its effect into account. In SMS this result has been achieved through the implementation of the unified formulation of damper load. In particular, a correction which is a function of damper load and modal data is calculated in flat, edge and torsion and subtracted from the bending gauge data before the elastic mode fitting process is completed.

Concerning the mentioned limitations about radial components, some additional terms, analytically generated by using hub accelerations and blade lagging velocity, have been taken into account in the calculation of longitudinal and lateral shears.

Hub acceleration has been directly measured by means of an installed sensor, while lagging velocity has been derived by processing the information about blade motions (a dedicated tool, designed for measuring in-flight blade angles, has been used for this purpose).

Further correction on the unknown radial shear quantity is that arising from resolution of the aerodynamic lift loads, resolved through the local blade flapping angle. The latter parameter can be estimated from a reconstruction using SMS modal responses and modal blade. In the absence of a pressure

gauged blade, the lift has been estimated using a novel process developed by AgustaWestland, which derives lift loads from blade strain gauge data.

HUB LOADS COMPARISON

Starting from beam and chord forces at the reference blade hinge, it has been possible to evaluate the resulting forces and moments acting at hub centre by applying the following steps:

- calculation of the resulting hub loads in the rotating frame, in terms of main harmonic contributions, due to beam and chord forces at blade hinges (for the all the N blades);
- calculation of the corresponding hub loads in the fixed frame (static and N/rev);
- correction of the in-plane shear basing on the contributions due to the inertial force of the hub and to the M/R dampers force (not included in blade hinge loads elaboration), in order to compare the resulting hub loads with the corresponding ones obtained by processing the mast bending data.

The following diagrams show the comparison, for the 6 hub loads, between mast (red curves), hub (black color) and blades (green color) elaborations.

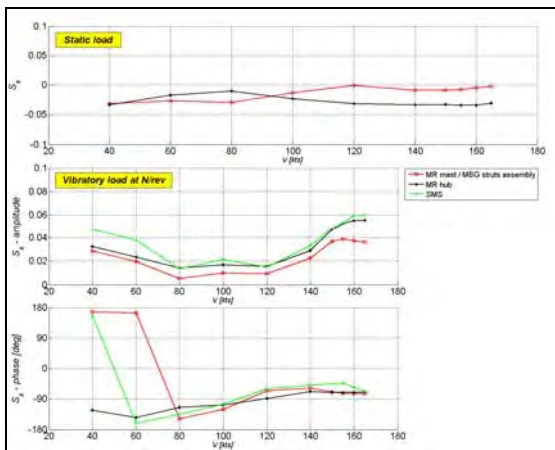


Figure 8: Fore-aft hub forces comparison

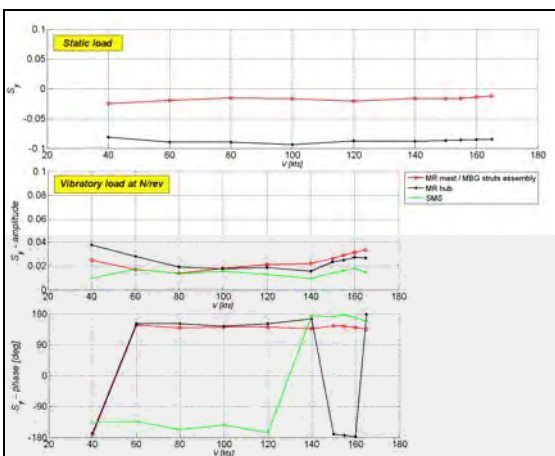


Figure 9: Lateral hub forces comparison

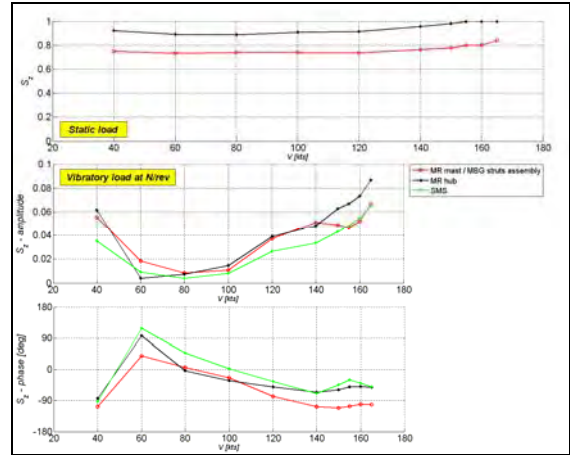


Figure 10: Vertical hub forces comparison

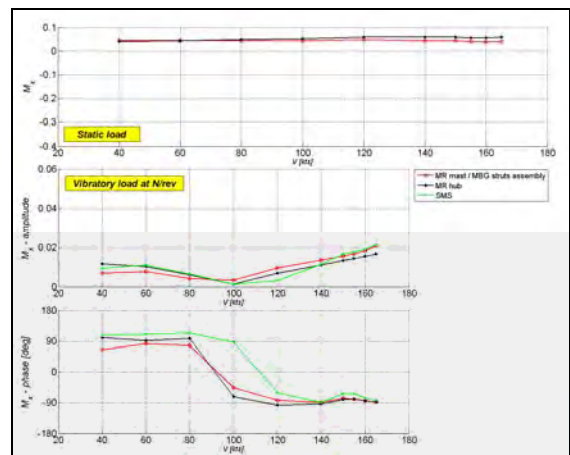


Figure 11: Roll hub moments comparison

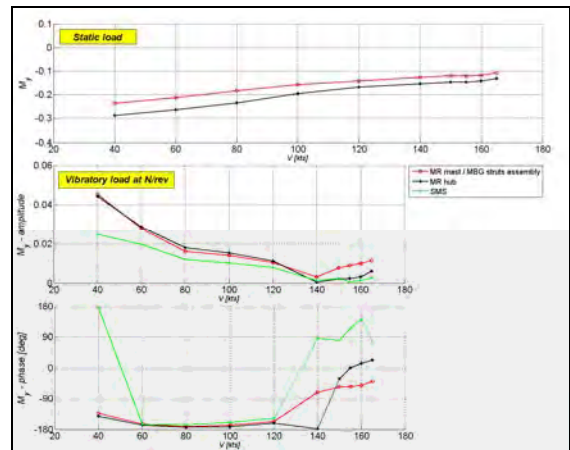


Figure 12: Pitch hub moments comparison

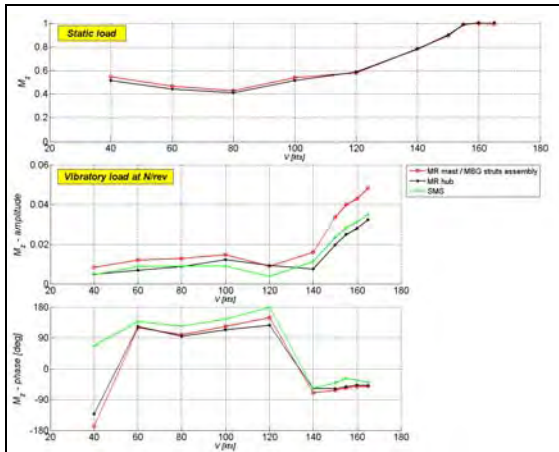


Figure 13: Torque hub moments comparison

In general, good agreement can be highlighted between SMS/hub derived thrust, roll, pitch and torque moments (both static and vibratory) and those obtained from mast/MGB methodology (except for static thrust that seems to be moderately overestimated by hub method). This level of agreement between completely independent methods gives a high level of confidence, for the selected loads, in the values thus obtained.

On the contrary, the agreement between the values related to the in plane shears are not as satisfactory, although the compared loads exhibit the same order of magnitude and similar trends (except for the lateral static shear that seems to be largely underestimated by hub procedure).

The good level of agreement between thrust and moments, for the three calculation procedures, would tend to indicate that the radial force could be the main cause of the noted discrepancies, especially considering that:

- SMS method is incapable of accounting for radial shear, which is subsequently added in the calculation, as explained before;
- M/R hub procedure does not take into account the possible contribution of the radial force on the strain gauges measurements for test rig limitations;
- the best comparison found refers to the loads which have more influence in BBl measurements, probably less affected by radial forces; moreover, the good reconstruction related to static and N/rev components of CB measurements (not affected by radial loads), led to a satisfactory comparison for torque moment, which is the corresponding load.

HINGE FORCES COMPARISON

The following figures show a comparison between hub (black curves) and blade (red curves) elaboration in terms of flap and lag forces at reference blade hinge. In particular, the comparison is focused on the main harmonic components in the rotating frame $\{(N-1)/rev, N/rev \text{ and } (N+1)/rev\}$.

Concerning the meaning of the mentioned blade hinge forces, these refer to the all loads coming from main rotor blades and so include:

- aerodynamic forces
- blades inertial contribution

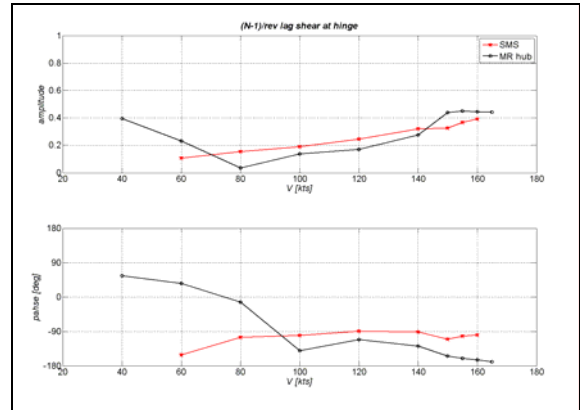


Figure 14: lag hinge forces - $(N-1)/rev$ component

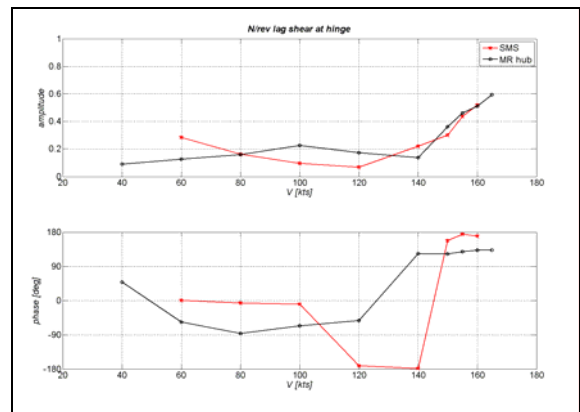


Figure 15: lag hinge forces - N/rev component

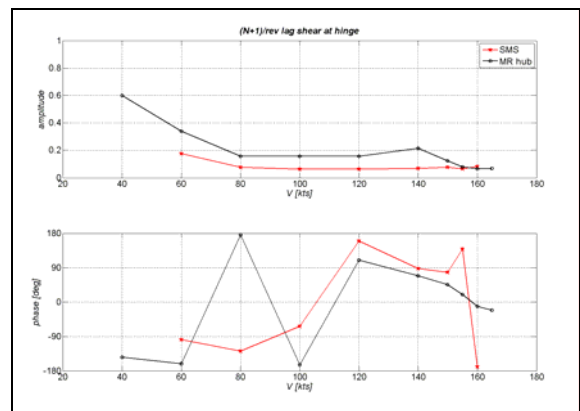


Figure 16: lag hinge forces - $(N+1)/rev$ component

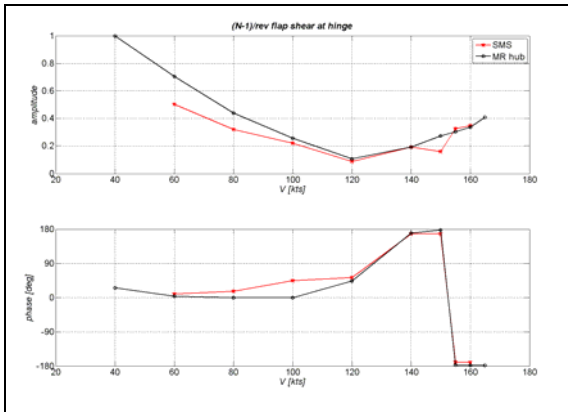


Figure 17: flap hinge forces - $(N-1)/rev$ component

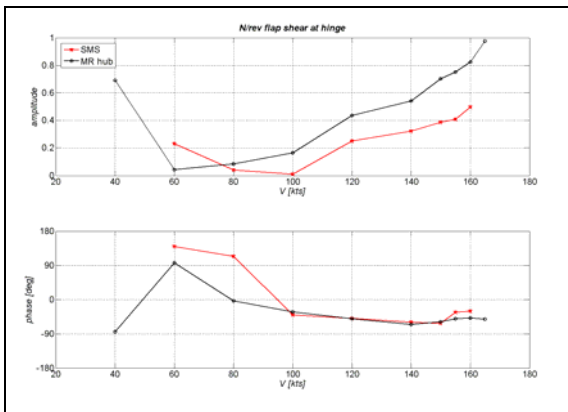


Figure 18: flap hinge forces - N/rev component

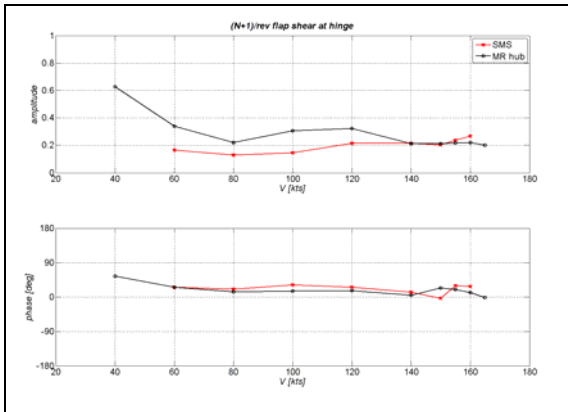


Figure 19: flap hinge forces - $(N+1)/rev$ component

In general, a quite good agreement can be highlighted between the results obtained by using the two calculation methods, except for N/rev component of the flap hinge force at high flight speed.

The following considerations can be done by observing these diagrams:

- for the high speed flight conditions, the harmonic components at $(N-1)/rev$ and N/rev represent the main contributions for the lag and flap force at blade hinge
- for the low speed flight conditions, all main harmonic components provide a significant

contribution to the blade hinge forces, except for what concern the N/rev lag harmonic which is significantly lower than the other ones

ROTOR LOADS SUMMARY

Hub loads summary, resuming the results obtained by applying mast/MGB assembly methodology, is shown in the following diagrams.

The choice of using this approach, in place of the other two methods for inferring the final rotor loads in the fixed frame, is based on the more completeness of the related results, as well as the improved robustness of its calculation. Notice that the results refer to all loads coming from main rotor blades, including *pitch links* forces.

For more clarity, the curves plotted in all the diagrams are grouped by colour, according to the flight configuration (Weight and C.G.) characteristics, described below:

- Red line - Maximum weight, C.G. AFT
- Green line - Intermediate weight, C.G. AFT
- Blue line - Maximum weight, C.G. FWD

Flights with the same colour have identical configuration, providing a substantiation of the repeatability of the methodology.

The figures show both static (on the top) and N/rev vibratory load components (on the bottom).

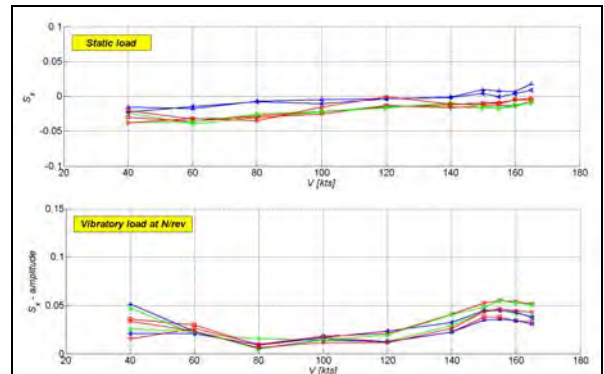


Figure 20: Fore-aft rotor forces summary

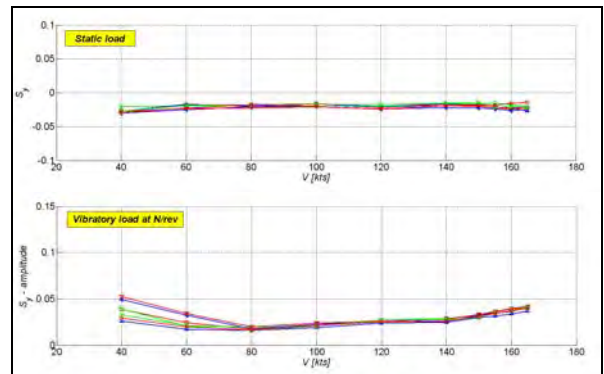


Figure 21: Lateral rotor forces summary

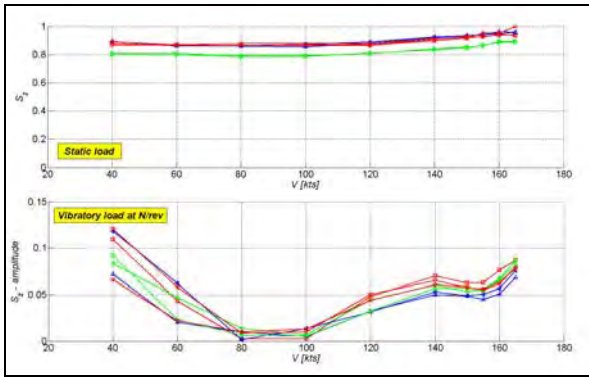


Figure 22: Vertical rotor forces summary

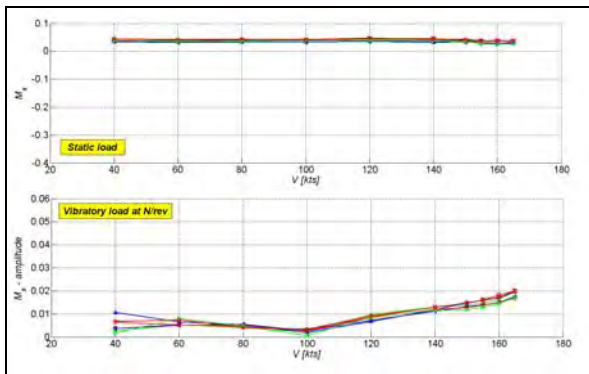


Figure 23: Roll rotor moments summary

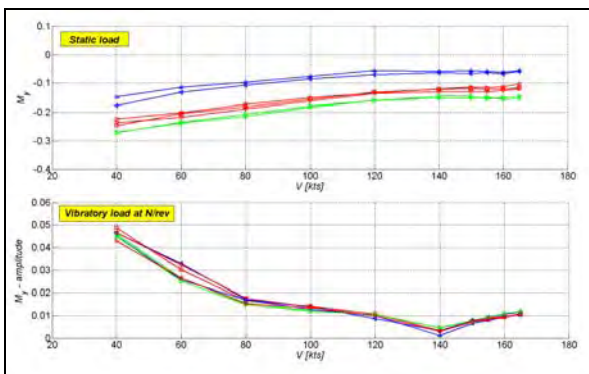


Figure 24: Pitch rotor moments summary

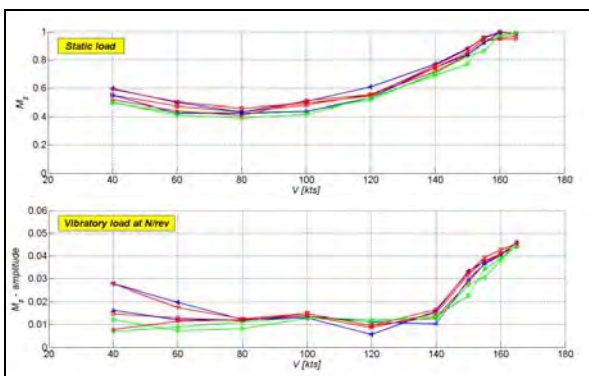


Figure 25: Torque rotor moments summary

For what concern vibratory loads, the results appear to be quite comparable and the differences are most evident in

thrust loads comparison and confined prevalently at low speeds.

About static loads, the following observations can be highlighted:

- static trends are similar, comparing different flights, and are grouped according to the different helicopter configurations flown;
- the in-plane loads (shears and moments) seem to be mostly affected by C.G. configuration, while thrust forces, as expected, are more dependent from helicopter weight;
- the variation of static thrust is consistent with the helicopter weight change.

CONCLUSIONS

The methodology illustrated in this paper has the scope to find out a valid procedure to obtain an accurate measurements of the complete loads set, both static and dynamic, coming from the main rotor.

The employment of different measurements on multiple structural load paths (mast, hub and blade instrumented components) allowed to calculate and then validate the complete set of hub loads.

Moreover, the accuracy and robustness of the results have been increased by using some improvements about the employed instrumentation and on the definition of new calibration/sensitivity tests.

In general, good agreement can be highlighted between SMS/hub derived thrust, roll, pitch and torque moments (both static and vibratory) and those obtained from mast/MGB methodology. This level of agreement between completely independent methods gives a high level of confidence, for the selected loads, in the values thus obtained. On the contrary, the agreement between the values related to the in plane shears are not as satisfactory, although the compared loads exhibit the same order of magnitude and similar trends. These remarks would tend to indicate that the radial force could be the main cause of the noted discrepancies.

On this subject, an experimental calibration of the M/R hub strain gauges with respect to this type of load or a better implementation of the radial terms in the SMS procedure, could provide in the future some improvements in the results based on hub/blade data.

Concerning the vibratory forces at blade hinge, two completely independent elaboration procedures (SMS and hub data methods) provided quite similar results, both in terms of amplitudes (magnitude and trend with respect to flight speed) and phases. Thus confirming the robustness of the obtained results.

References

[1] Bielawa, Richard L., "Rotary wing structural dynamics & aeroelasticity" Second Edition, AIAA, 2002

[2] Johnson, Wayne, "Helicopter theory", Princeton University Press, 1980